COMPARISONS OF DIFFERENT ELECTROMAGNETIC SOLVERS FOR ACCELERATOR SIMULATIONS[*]

J. Xu[†], X. Zhufu, R. Zhao, Institute of Software, Beijing, 100190, China

C. Li, X. Qi, L. Yang, Institute of Modern Physics, Lanzhou, 730000, China

M. Min, Argonne National Laboratory, Argonne, IL 60439, USA

Abstract

Electromagnetic simulations are fundamental for accelerator modeling. In this paper two high-order numerical methods will be studied. These include continuous Galerkin (CG) method with vector bases, and discontinuous Galerkin (DG) method with nodal bases. Both methods apply domain decomposition method for the parallelization. Due to the difference in the numerical methods, these methods have different performance in speed and accuracy. DG method on unstructured grid has the advantages of easy parallelization, good scalability, and strong capability to handle complex geometries. Benchmarks of these methods will be shown on simple geometries in detail first. Then they will be applied for simulation in accelerator devices, and the results will be compared and discussed.

INTRODUCTION

Time dependent electromagnetic simulations are bases for many accelerator simulations. It is an important area in computational electromagnetics. Many numerical methods have been developed till now, such as finite difference (FDM), finite volume (FVM) and finite element methods (FEM). FEM has the advantage of handling complex geometries, therefore many efforts have been made with FEM. For FEM methods, there are two types of methods have been proved successful, they are CG with vector base and DG with Nodal base. In this paper we will study the performance of these two methods.

The paper is organized in the following way: the numerical method is explained and algorithms are compared in section 2, validation is shown in section 3, then benchmarks results are shown in section 4, and a comparison on wakefield simulations is given in section 5. At last, the conclusion is drawn in section 6.

NUMERICAL METHOD

Maxwell's Equation

In 3D domain Ω, time dependent Maxwell's equations can be written as:

$$\frac{\partial \mathbf{B}}{\partial \mathbf{t}} = -\nabla \times \mathbf{E}, \qquad \frac{\partial \mathbf{D}}{\partial \mathbf{t}} = \nabla \times \mathbf{H} + \mathbf{J} \qquad (1)$$

$$\nabla \cdot \mathbf{D} = \rho, \qquad \nabla \cdot \mathbf{B} = \mathbf{0}, \quad \mathbf{x} \in \mathbf{\Omega}, \qquad (2)$$

$$\hat{\mathbf{n}} \times \mathbf{E} = \mathbf{0}, \qquad \hat{\mathbf{n}} \cdot \mathbf{H} = \mathbf{0} \quad \mathbf{x} \in \partial\mathbf{\Omega}, \qquad (3)$$

where, the electric field $\mathbf{E}$, electric flux density $\mathbf{D}$, as well as the magnetic field $\mathbf{H}$ and the magnetic flux density $\mathbf{B}$ are related through the constitutive relations $\mathbf{D} = \epsilon\mathbf{E}, \mathbf{B} = \mu\mathbf{H}$.

CG Formulation

Maxwell's Equation (1) can be written in following inhomogeneous wave equation

$$\nabla \times \frac{1}{\mu_r}\nabla \times \mathbf{E} + \frac{\epsilon_\mathbf{r}}{\mathbf{c_0^2}}\frac{\partial^2 \mathbf{E}}{\partial \mathbf{t^2}} = -\mu_\mathbf{0}\frac{\partial \mathbf{J}}{\partial \mathbf{t}} \qquad (4)$$

which times edge bases and apply electric (PEC) boundary condition to arrive at

$$\mathbf{M}\frac{\mathbf{1}}{\mathbf{c_0^2}}\frac{\mathbf{d^2 e}}{\mathbf{dt^2}} + \mathbf{Se} = -\vec{\mathbf{f}} \qquad (5)$$

where $\mathbf{M}$ and $\mathbf{S}$ are mass and stiffness matrices in the following

$$\mathbf{M_{ij}} = \int_\Omega \epsilon_r \vec{W}_i \cdot \vec{W}_j d\Omega \qquad (6)$$

$$\mathbf{S_{ij}} = \int_\Omega \frac{1}{\mu_r}\nabla \times \vec{W}_i \cdot \nabla \times \vec{W}_j d\Omega \qquad (7)$$

$$f_i = \int_\Omega \mu_0 \vec{W}_i \cdot \frac{\partial \vec{J}}{\partial t} d\Omega \qquad (8)$$

Based on the Newmark-Beta formulation [1, 2], Equation (5) can be solved to obtain e^{n+1} with

$$\begin{aligned}
e^{n+1} = {} & (M + \beta(c_0\delta t)^2 S)^{-1} \cdot \\
& \{(2M - (1 - 2\beta)(c_0\delta t)^2 S)e^n \\
& -(M + \beta(c_0\delta t)^2 S)e^{n-1} \\
& (c_0\delta t)^2(\beta f^{n+1} + (1 - 2\beta)f^n + \beta f^{n-1})\}
\end{aligned} \qquad (9)$$

More detailed information can be found in [1, 2, 3]. The CG method is based on Nédélec edge bases, which is explained in detail in [4], and we omit it due to the constraint of page limit.

DG Formulation

The discrete form of DG is:

$$\frac{\mathbf{dE_N}}{\mathbf{dt}} = \mathbf{M^{-1}S} \times \mathbf{H_N} + \mathbf{S^E}$$

$$+ \quad \mathbf{M}^{-1}\mathbf{F}(\hat{\mathbf{n}} \times \frac{\mathbf{Z}^{+}[\mathbf{H_N}] - \hat{\mathbf{n}} \times [\mathbf{E_N}]}{\mathbf{Z}^{+} + \mathbf{Z}^{-}})\Big|_{\partial \mathbf{D}} \quad (10)$$

$$\frac{\mathbf{dH_N}}{\mathbf{dt}} = \mathbf{M}^{-1}\mathbf{S} \times \mathbf{E_N} + \mathbf{S^H}$$

$$+ \quad \mathbf{M}^{-1}\mathbf{F}(\hat{\mathbf{n}} \times \frac{\hat{\mathbf{n}} \times [\mathbf{H_N}] + \mathbf{Y}^{+}[\mathbf{E_N}]}{\mathbf{Z}^{+} + \mathbf{Z}^{-}})\Big|_{\partial \mathbf{D}} \quad (11)$$

where $\hat{\mathbf{n}}$ is the normal vector on boundary, ϕ is the test function in Ω. $[\mathbf{E_N}] = \mathbf{E_N^+} - \mathbf{E_N^-}$ and $[\mathbf{H_N}] = \mathbf{H_N^+} - \mathbf{H_N^-}$ for the solutions $\mathbf{E_N^-}$ and $\mathbf{H_N^-}$ in the local domain and $\mathbf{E_N^+}$ and $\mathbf{H_N^+}$ in neighboring elements. M, S are mass and stifness matrixes respectively.

More details on DG method and nodal base Finite Element method can be found in [5, 6, 7, 8, 9], which also be skipped due to the page limit.

We adopt low-storage five-stage fourth-order explicit Runge-Kutta (LSERK) scheme has been used [5].

Methods Comparison

- As the order of the vector base is the order of nodal base minus 2, they have different accuracy for the interpolation, derivative and curl operators.
- Total degree of freedom when using CG with vector base is much less than the total degree of freedom when using DG nodal base.
- Both algorithms solve the Maxwell's equation in time domain, but since the CG method use nodal base, it has no extra cost for transforming the fields to the spectral space.
- CG method needs to inverse global matrixes, while DG method only needs to inverse local matrixes. This makes the DG method to have better scalability and faster speed.
- DG method need to exchange face information for each element, this usually needs more memory and the communication is more than CG method.
- DG method uses 4th order Runge-Kutta integration scheme, while CG method uses 2nd order time integration scheme.

VALIDATION

Analytical Solution

In order to further verify our results in 2D case, we conduct similar tests in 3D. The analytic solution with periodic boundary condition in $[-\pi, \pi]^3$ are:

$$E_x = 0.0$$
$$E_y = \cos(x) \cdot \sin(y) \cdot \sin(z) \cdot \cos(\sqrt{3}t)$$
$$E_z = \cos(x) \cdot \cos(y) \cdot \cos(z) \cdot \cos(\sqrt{3}t)$$
$$H_x = 2.0 \cdot \cos(x) \cdot \sin(y) \cdot \cos(z) \cdot \sin(\sqrt{3}t)/\sqrt{3}$$
$$H_y = -\sin(x) \cdot \cos(y) \cdot \cos(z) \cdot \sin(\sqrt{3}t)/\sqrt{3}$$
$$H_z = \sin(x) \cdot \sin(y) \cdot \sin(z) \cdot \sin(\sqrt{3}t)/\sqrt{3}$$

Table 1: Comparison of DOFs (E=203)

Polynomial Order	3	4	5
CG vector base	165	1038	3231
DG nodal base	4902	10184	18310

$$(12)$$

The errors verses time have been plotted in Fig. 1. As can be seen that the errors with both method decrease as polynomial order increases. Since the order of the vector base (PM) equals the order of nodal base (P) minus 2, for the same P, the error of vector base is larger than the nodal base. Another difference is the errors for the DG method oscillate around a constant level, while the errors for the CG method increase linearly.
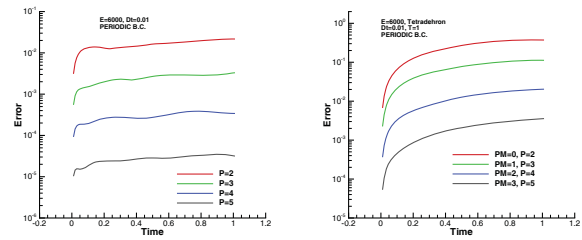

Figure 1: Errors versus polynomial orders: Nodal base (left); vector base (right)

BENCHMARKS

In order to compare performance in detail, we study them in following different perspectives.

Degree of Freedom

First we compare degrees of freedom in Table 1, as can be seen that DOF of vector is much less than the DOF of nodal base. This makes the size of global mass and stiffness matrices smaller when using vector base than using nodal base. This usually leads to better condition number for the matrix and can achieve fast speed. As DG method been used instead of CG, inverse of global matrix has been avoided which eliminate this shortcoming.

Iteration Convergence Speed

In order to see the differences of speed with different vector base orders, the comparison has been given in Table 2. From the table, the increase of time is nonlinear. This make it difficult to use for higher order vector base.

Speed Comparison

Next, we compare their speeds with 6000 tetrahedra and running for T=1. Currently CG solver has not been fully optimized. Table 3 shows that for P=2 (PM=0), CG with

Table 2: Iteration Steps for Inverse Operation with Vector Base (E=6000)

Nodal Base Order (P)	2	3	4
Vector Base Order (PM=P-2)	2	3	4
Iteration steps	36	111	276

Table 3: Comparison of Speeds (E=6000)

Nodal Base Order	2	3	4	5
DG Nodal Base	6.35	14.1	24.3	46.1
Vector Base Order	0	1	2	3
CG Vector Base	2.14	32.86	333.95	2561.78

vector is faster. When P larger than 2, DG with nodal base is faster. As the inverse takes more and more time, the speed for CG with vector base increase nonlinearly and this is a big challenge for using CG method.

Comparison of Wakefield Simulations

We have used these two solvers for a wakefield simulation. A Gaussan beam has been simulated in the device shown in Fig. 3 . The longitudinal wake potential has been calculated at r=1 for different beam bunch sizes, $\sigma_z = 0.25, 0.5, 0.75, 1.0$ and $\sigma_r = 0.1$. A 2D poisson equation has been solved to get the initial electric field and current has been activated to simulate the charged beam.

Left plot in Fig. 2 shows the wakepotential comparison. Solid line is the result using DG nodal base, and dash line is the result for CG vector base. They are consistent, this means both solvers produce correct results and they both can be used for the wake field simulations. The right one shows the beam distribution function for different $\sigma_z = 0.25, 0.5, 0.75, 1.0$.
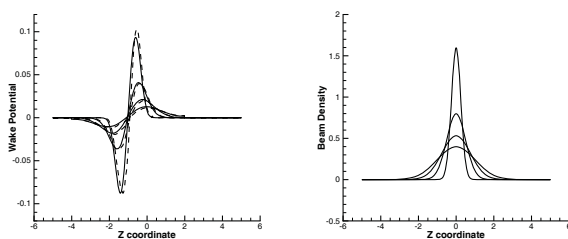

Figure 2: Comparison of wakepotential(left: Nodal base-solid, vector base-dash); beam distribution for (σ_z=0.25,0.5,0.75,1.0)

Figure 3 shows the electric field contours from the simulation. Totally 561883 tetrahedra elements have been used, and P=2.

CONCLUSION

In this paper, we have compared performance of two types time dependant EM solvers. They both can be used
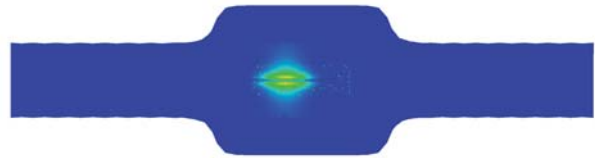

Figure 3: Contour of electric field

for accelerator simulations. Comparisons have been performed in terms of DOFs, iteration steps, accuracy, and speed. At last, results for a wakefield simulation has been compared. CG method with vector base has smaller DOFs than CG with nodal base, but due to the nature of solving global matrix, CG method with vector base has the challenge when DOF becomes large. On the other side, the memory cost of DG is much larger than CG method, which is a challenge for DG method.

ACKNOWLEDGMENT

REFERENCES

[1] N. M. Newmark, A method of computation for structural dynamics, Journal of Eng. Mech. Div., ASCE, vol. 85, pp. 67-94, July 1959.

[2] O.C. Zienkiewicz, A new look at the Newmark, Houboult and other time stepping formulas. A weighted residual approach., Earthquake Engineering and Structural Dynamics, vol. 5, pp. 413-418, 1977.

[3] A. Candel, A. Kabel, L. Lee, Z. Li, C. Limborg, and C. Ng, Parallel 3D Finite Element Particle-In-Cell Code for High-Fidelity RF Gun Simulations, Proceedings of LINAC08, Victoria, BC, Canada, 2008.

[4] J. Jin, The Finite Element Method in Electromagnetics, second edition John Wiley & Sons, Inc., New York, (2002).

[5] J.S. Hesthaven and T. Warburton, Nodal Discontinuous Galerkin Methods: Algorithms, Analysis and Applications, Springer, New York, (2008).

[6] M. Min, P.F. Fisher, and T. Chae, Spectral Element Discontinuous Galerkin Simulations for Wake Potential Calculations: NEKCEM, Proceedings of PAC07, Albuquerque, New Mexico, USA, 2007.

[7] M. Dubiner, Spectral Methods on triangles and other domains, *J. Sci. Comp.*, **6**, 345, (1991).

[8] T. Koornwinder, Two-variable analogues of the classical orthogonal polynomials, in *Theory and Applications of Special Functions*, edited by A.R.A. (Academic Press, San Diego, 1975).

[9] W.H. Reed and T.R. Hill, Triangular mesh methods for the beutron transport equation, Tech. Report LA-UR-73-479, Los Alamos Scientific Laboratory, Los Alamos, NM, 1973.